Structure Dimensions Variation of the Segmented Switched Reluctance Linear Synchronous Motor (SSRLSM) and the Effect on Its Performances

Nur Ashikin Mohd Nasir†, **Fairul Azhar Abdul Shukor**, **Norrimah Abdullah**, and **Raja Nor Firdaus Kashfi Raja Othman**, Non-members

ABSTRACT

This paper proposed and discussed a SRLSM with the segmental pole. The segmented SRLSM which known as SSRLSM was designed for domestic lift application. The SSRLSM was designed to fulfill the design target requirement where the lift must be able to transport a maximum 200 kg payload. A lab-scaled prototype of the SSRLSM was developed for experimental and measurement purpose. Beforehand, the SSRLSM was designed and simulated for different structure dimension to study the effect of structure's reduction towards its performances. The structure dimensions involved are the number of coil number and the stack length where the number of coil is reduced from 6 coils to 3 coils. The results show that the thrust produced by the 6-coils and 3-coils SSRLSM is 2400 N and 1200 N, respectively. This shows that, the thrust is reduced by 50 % as the number of coil reduced by half. At the same time, the thrust produced also reduced by approximately 50 % as the stack length, z reduced by half from 400 mm to 200 mm. This shows that, the thrust, F of the SSRLSM is directly proportional to the number of coil as well the stack length, z.

Keywords: Domestic Lift, Linear Motor Lift System, Linear Switched Reluctance Motor, Segmented SRLSM, Stack Length, Structure Dimension

1. INTRODUCTION

In recent years, the switched reluctance linear synchronous motors (SRLSMs) are being increasingly advocated as an alternative to other linear electrical motors such as linear induction motor (LIM) and permanent magnet linear synchronous motor (PMLSM) in many applications [1], [2], [3]. This is cause by their simple and robust construction with concentric windings on only one side which is stator or translator, and fault tolerance due to absence of mutual coupling between windings, maintenance ease, less thermal problems and cooling arrangement, and finally low-cost [4]. With these advantages, the SRLSMs have been studied as to their suitability in some linear applications such as in horizontal linear transportation system, high-precision position application in the manufacturing automation and cylindrical type linear actuator using an SRLSM for applications requiring controlled low-speed linear motion [4].

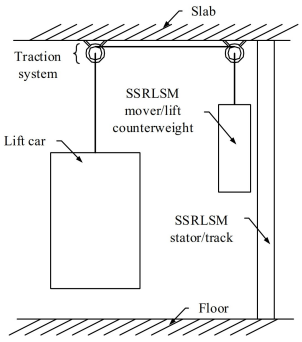

***Fig. 1**: Skeleton of the SSRLSM Domestic Lift.*

In this research, a SSRLSM for domestic lift was proposed in a laboratory scale for preliminary study and proof of concept. Fig. 1 shows the skeleton of the proposed SSRLSM domestic lift. It is a traction lift system where the SSRLSM acts as the actuator as well as a counterweight. This type of lift system is deliberately able to minimize the installation space consumed since the complex mechanical systems of the conventional lift systems were reduced [5]. The domestic lift was designed to be able to transport maximum two people at a time with maximum pay load; 2 people and luggage is 200 kg [6]. Therefore, it requires a motor with the thrust, F more than 2000 N [6].

2. SEGMENTED SWITCHED RELUCTANCE LINEAR SYNCHRONOUS MOTOR

2.1 Basic Structure of the SSRLSM

In this research, the SRLSM is designed using segmented-type structure. Compare to the conventional SRLSM, the segmented SRLSM was designed without

Manuscript received on August 15, 2023; revised on July 31, 2024; accepted on August 1, 2024. This paper was recommended by Associate Editor Matheepot Phattanasak.

The authors are with Faculty of Electrical Engineering, Universiti Teknikal Malaysia Melaka (UTeM), Hang Tuah Jaya, Durian Tunggal, 76100 Melaka, Malaysia.

†Corresponding author: nurashikinmohdnasir@gmail.com

Digital Object Identifier: 10.37936/ecti-eec.2024223.248392

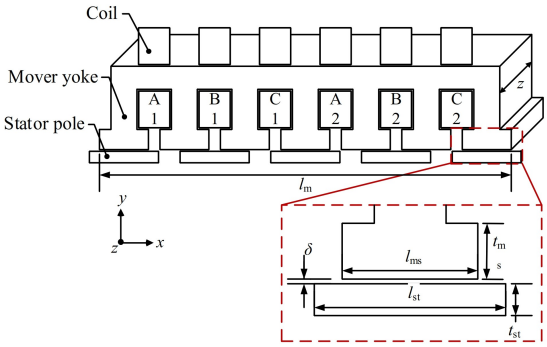

***Fig. 2**: Basic Structure of the SSRLSM.*

***Table 1**: Parameters Specification of the SSRLSM.*

Parameter	Value
Stack length, z	400 mm ~ 40 mm
Air gap length, δ	3 mm
Mover shoe length, l_{ms}	85 mm
Mover shoe thickness, t_{ms}	35 mm
Mover total length, l_m	715 mm
Stator pole length, l_{st}	120 mm
Stator pole thickness, t_{st}	20 mm
Number of coil	6 & 3
Number of turns, N	1800
Winding resistance, R	20 Ω

teeth on both mover and stator side. The purpose of the shape is to minimize the effect of manufacturing tolerance [7] as well as increase the efficiency of the motor performance. Apart from that, by adopting a segmental structure, the SSRLSM produce higher thrust density compared with the conventional SRLSM with the similar dimensions [8]. Fig. 2 shows the basic structure of the 3 phase 6-slot 4-pole SSRLSM. The SSRLSM is designed in a flat structure. The mover consist of yoke and coil meanwhile the stator consists of segmental stator pole. The material for the stator pole and stator yoke is SS400. Table 1 shows the specification of the SSRLSM.

2.2 Basic Thrust Equation of the SSRLSM

In the SSRLSM, the thrust is developed based on the principle of variable reluctance [9] related to the excited mover coil and the magnetic flux lines. Due to the dependence of magnetic flux line distribution and magnetic induction on the excited phase position in linear motors, the FEM results are focused on Phase B. This phase experiences minimal influence from end effects, enabling the analysis of the motor's behaviour with minimal distortion caused by these non-uniformities. Fig. 3 shows the magnetic flux lines of the SSRLSM when the coil of the Phase B is excited. Once excited, the flux lines from the excited mover goes through the mover yoke, passing through air gap and stator pole then return the mover yoke to complete a close path. At the fully unaligned position as shown in Fig. 3 (a), the flux lines flow between

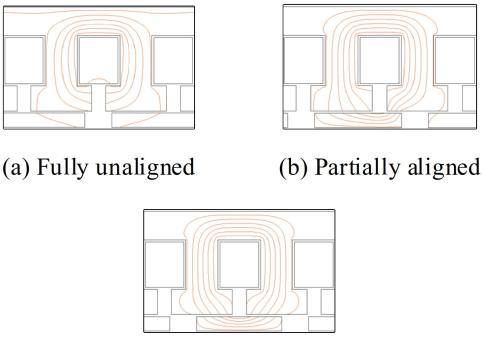

(a) Fully unaligned (b) Partially aligned

(c) Fully aligned

***Fig. 3**: SSRLSM Magnetic Flux Lines (I = 2.5 A).*

two stator poles where both stator poles are magnetically isolated from each other. The space between the stator poles plays a role as the magnetic reluctance [10]. The magnetic reluctance will moves the mover pole to align with the stator pole. Therefore, at the partially aligned position; Fig. 3 (b), where the flux lines are partially passing through the stator pole to enclose the path, the thrust, F is developed as the mover pole tries to align with the stator pole. In Fig. 3 (c), once the mover pole is fully aligned with stator pole, the excited mover slot is enclose magnetically as the flux lines complete the close path. At this point, the magnetic reluctance is minimum.

Apart from that, the general thrust, F of the SSRLSM can be expressed as Eq. (1) [6], [11]. Where F is thrust in (N), I is the input current in (A), n is the Fourier order, Φ_n is nth Fourier component of magnetic flux in (Wb), τ_p is pole pitch in (m) and x is the stator displacement in (m). Based on Eq. (1), it shows that, the thrust, F of the SSRLSM is depends on coil parameter such as coil turns, N and current, I, as well as pole pitch, τ_p.

$$F = -NI\sum_{n=1}^{\infty}\Phi_n \sin\left[\frac{2\pi}{\tau_p}nx\right]\frac{2\pi n}{\tau_p} \qquad (1)$$
$$= -\frac{2\pi NI}{\tau_p}\sum_{n=1}^{\infty} n\Phi_n \sin\frac{2\pi}{\tau_p}nx$$

2.3 Effect of Structure Dimension towards Thrust, F Performance

In motors design, the geometry structure dimensions and the number of rotor poles play a crucial part in the performances of the motor. This condition can be related to the electromagnetic circuit of the motors hence affected the motors performances [12]. Therefore many researchers [13-14] study the effect of motors geometry structures towards their performances. One of the performances studied by the researchers is the torque production.

In rotational motor, the torque, τ produced by a motor can be related to the diameter, d and the stack length, $z$of the motor. This condition is expressed in Eq. (2).

$$\tau \propto r^2,\ z \tag{2}$$

where τ is torque in Nm, r is the radius of the motors in mm, and z is the stack length of the motor in mm. Based on this expression, it can be assumed that the relationship between torque and stack length, z as well as motor diameter, d is directly proportional. The increasing in stack length, z or the diameter, d of the motor will increase the torque produced. Apart from that, in the study conducted by [15-16], the authors concluded that the torque developed by a motor is similar as long as the total number of turns of the motor is kept constant regardless of the number of phase. It is also stated that the increasing in the number of phase of the motor does not affected the magnetic flux density, $\boldsymbol{B}_g$ at the air gap region.

However, in the linear motors, due to their open structure and finite length, the relationship might not be similar to the rotational motors. Besides that, there are not many literatures can be found regarding the relationship between the stack lengths, z and the thrust, F production. Therefore, the aforementioned relationships was studied and presented in this paper to estimate the lab-scaled prototype for the domestic lift performances.

3. VARIATION OF THE SSRLSM STRUCTURE PARAMETERS

Previously, the SSRLSM has been designed and discussed in [6]. The optimum model determined was selected for fabrication. However, as a preparation to preliminary study and proof of concept, as well as to encounter any mechanical issues such as linear motion mechanism and alignment, a lab-scaled prototype was built instead of full-scaled prototype. The lab-scaled prototype was built to a scale quarter of the original scale. On the other hand, before fabricating the lab-scaled prototype, the effect of scaling down the structure is studied. This process is crucial in identifying the pattern of changes between the number of coils and stack length, z towards the thrust characteristics of the SSRLSM. In this matter, the performances of the SSRLSM are analysed whether it is linear or non-linear with the changes of the structure dimensions. The SSRLSM structure parameters involved are the number of coil and the stack length, z. The performances observed are thrust, F characteristics and the magnetic flux density, $\boldsymbol{B}$ profile.

Fig. 4 shows the process flow of the SSRLSM's structure reduction. The design start by determined the initial parameters of the SSRLSM based on the original model as in Table 1. The process continued by reducing the number of coil from six to three. In this process, the other structure parameters as well as the stack length, z are fixed. Apart from that, the number of turns, N and the value of resistance, R also fixed to 1800 and 20 Ω, respectively. The model was then simulated for thrust, F performance. The process continued by reducing the value of stack length, z to a few possible value. The values considered are 200 mm, 100 mm, and 40 mm which

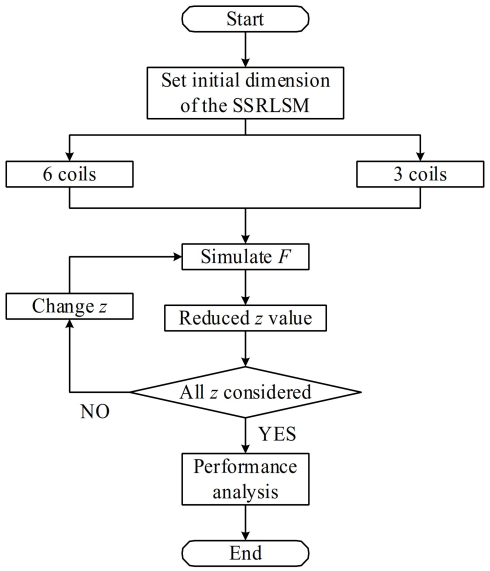

***Fig. 4**: Flowchart of the SSRLSM's Structure Reduction.*

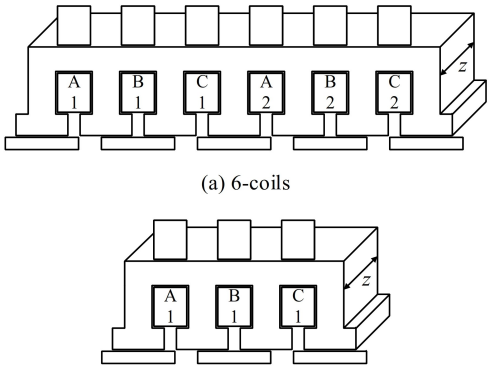

***Fig. 5**: SRLSM's Topology.*

respectively, are 50 %, 25 %, and 10 % of the original stack length, z value. Each model was then simulated with FEM software for thrust, F performances. The thrust, F performances obtained were analysed and compared.

4. EFFECT OF DIMENSION VARIATION TOWARDS SSRLSM PERFORMANCES

Fig. 5 shows the SSRLSM structure with different topologies which are 6-coils and 3-coils SSRLSM. The models of the SSRLSM from these two topologies and their variation of stack length, z are simulated by using FEM software. The simulation results obtained are analysed and compared.

4.1 Magnetic Flux Density, B Performance

Fig. 6 (a)-(c) shows magnetic flux density, $\boldsymbol{B}$, distribution for the SSRLSM at the excitation current, I of 2.5 A. The indigo colour shows the regions where the magnetic flux density, $\boldsymbol{B}$, is minimum. Oppositely, the red regions are the region with maximum magnetic flux density, $\boldsymbol{B}$. In

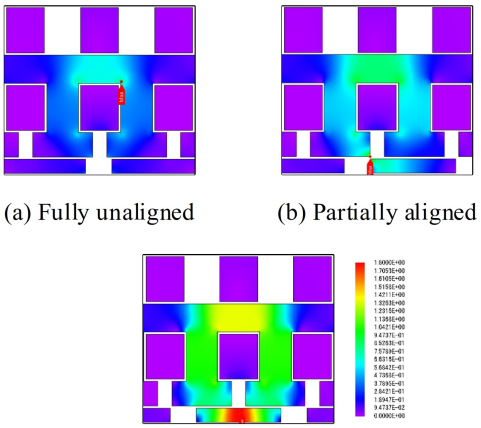

(a) Fully unaligned (b) Partially aligned

(c) Fully aligned

***Fig. 6**: SSRLSM Magnetic Density Contour (I = 2.5 A).*

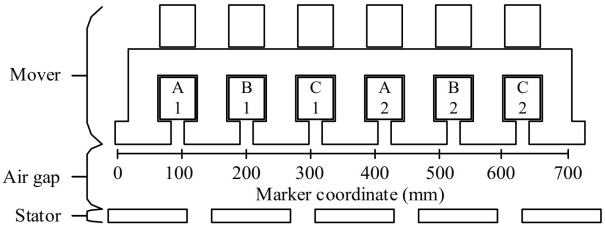

***Fig. 7**: Marker Coordinate at Air Gap Region (Not to Scale).*

Fig. 6 (a), where the SSRLSM at the fully aligned position, it can be observed that the magnetic flux density, $\boldsymbol{B}$, is high especially on the mover yoke region around excited coil. However, the maximum value can be observed on the stator pole region. In this condition, the maximum 1.8 T was recorded at the stator pole. Nevertheless, at the fully unaligned position as shown in Fig. 6 (c), the distribution of the magnetic flux density at the mover yoke is minimum and only concentrated at the upper region of the yoke where the value recorded is 1.13 T.

Based on the magnetic density, $\boldsymbol{B}$ contour as depicted in Fig. 6, the magnetic density, $\boldsymbol{B}_g$ distribution at the air gap region is extracted. The magnetic flux density, $\boldsymbol{B}_g$ distribution is plotted based on the marker coordination as illustrated in Fig. 7. Fig. 8 shows the aforementioned magnetic density, $\boldsymbol{B}_g$ profile of the air gap region. The magnetic density, $\boldsymbol{B}_g$ profile is taken where Phase B was excited at fully aligned position.

Fig. 8 (a)-(b) shows the magnetic density, $\boldsymbol{B}_g$ profile for SSRLSM with 6 coils. As Phase B excited, the magnetic flux will flow from coil B1 and B2 respectively. As B1 energized, the magnetic flux that flow produced magnetic density, $\boldsymbol{B}_g$ at the coordinate 100 mm to 300 mm. The positive value (100 mm to 200 mm) and negative value (200 mm to 300 mm) of the magnetic density, $\boldsymbol{B}_g$ indicates different direction of the magnetic flux flow. Meanwhile, the magnetic density, $\boldsymbol{B}_g$ distribution at coordinate 400 mm to 600 mm is produced as B2 energized. At the other coordinate apart from the mentioned coordinate, the value of the magnetic density, $\boldsymbol{B}_g$ is 0 T as there is no flux flows at the area. On the other hand, when the number of coils reduced from six to three, the cycle of the magnetic density, $\boldsymbol{B}_g$ profile is reduced to half as the excited phase only consist of one coil (B1) as shown in Fig. 8 (c)-(d). Moreover, the reduction in the number of coils and stack length, z does not affected the magnitude of the magnetic density, $\boldsymbol{B}_g$. Hence, it is expected that the thrust, F performances is influenced by the active area where the thrust, F is developed.

***Table 2**: Maximum Thrust of the SSRLSM for 6-coils and 3-coils Topologies.*

Stack length, z	No. of coil	Thrust, F	Active area of thrust, a_F	Thrust reduction
400 mm	6	2400 N	286 000 mm^2	50 %
	3	1200 N	160 000 mm^2	
200 mm	6	1200 N	143 000 mm^2	50 %
	3	600 N	80 000 mm^2	
100 mm	6	580 N	71 500 mm^2	48 %
	3	300 N	40 000 mm^2	
40 mm	6	230 N	28 600 mm^2	48 %
	3	120 N	16 000 mm^2	

4.2 Thrust, F Performance

Fig. 9 (a) and (b) show the thrust, F characteristics of the SSRLSM for 6-coil and 3-coil topology, respectively. The thrust, F characteristics are taken at different values of stack length, z for each of the topology. Based on Fig. 9, the effects of the number of coils and the stack length, z, on the production of the thrust, F is observed. This relationship is summarized in Table 2.

In overall, it shows that the thrust, F produced is reduced by approximately 50 % from 6-coil topology to 3-coil topology. This condition can be related to the number of turns for each coil. Since each coil have similar number of turns, therefore they have similar current, I flow in the coil hence the mmf for each coil is fixed. This is verified by the magnetic density, $\boldsymbol{B}_g$ profile in Fig. 8. Because of the fixed mmf, the total induced flux, $\boldsymbol{\Phi}$ expected to be the same. Apart from that, based on Eq. (1), the thrust, F of the SSRLSM is expressed as the summation of the total flux induced by the total number of coils. Consequently, by reducing the total number of coils by half, the thrust, F produced is estimated to be decreased by half.

On the other hand, the effect of the stack length, z reduction towards thrust, F performance can be related to the active thrust area, a_F. Since the value of stack length, z is reduced, thus, the total active thrust area, a_F where the thrust, F is developed expectedly to be decrease accordingly. The active thrust area, a_F of the SSRLSM is expressed as in Eq. (3).

$$a_F = l_m \times z \tag{3}$$

where a_F is active thrust area in mm^2, l_m is the total length of the SSRLSM in mm, and z is the stack length of the SSRLSM in mm. Since the thrust is developed based

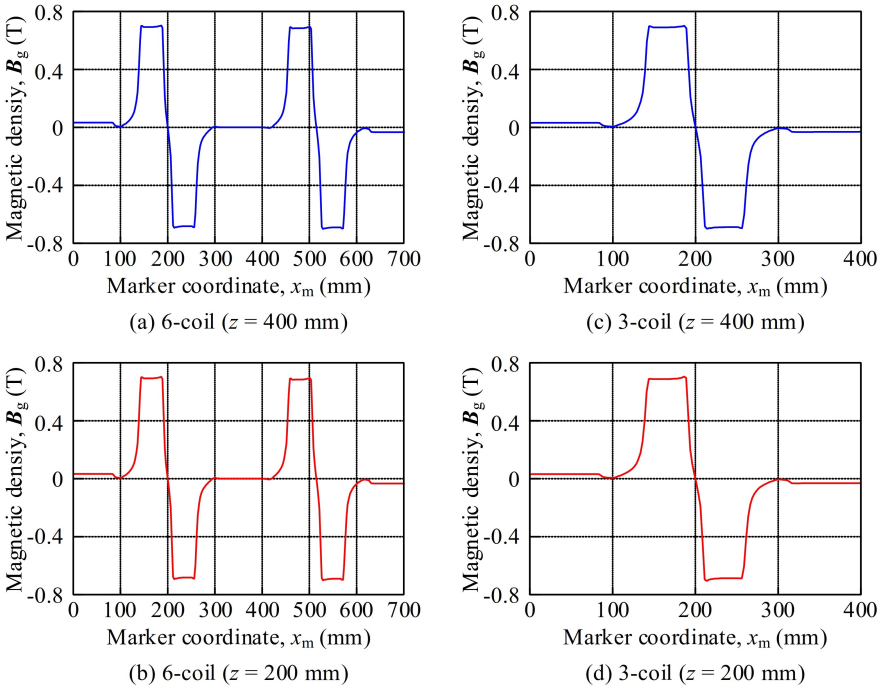

***Fig. 8**: SSRLSM magnetic flux density profile at fully aligned (I = 2.5 A).*

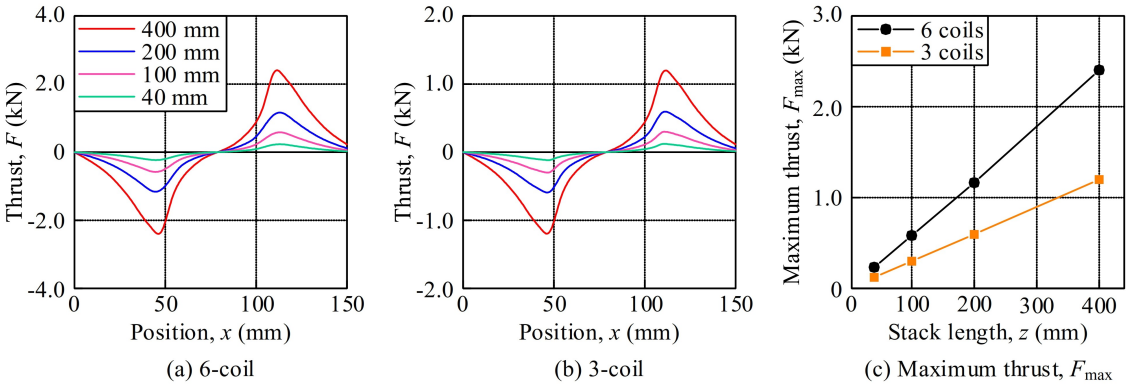

***Fig. 9**: SSRLSM thrust, F profile, I = 2.5 A.*

on this expression, the thrust, F characteristics shown in Fig. 9 (a)-(c) has proved this concept.

4.3 Thrust, F Validation

Based on the thrust, F performances shown in Fig. 9, a model was selected to be fabricated as a lab-scaled prototype for results validation. The selected model is the 3-coil topology with 200 mm of stack length, z. The domestic lift prototype was built with two sides of the SSRLSM. The prototype was assembled where the coil of each phases of each sides were connected in series and the measurement for static thrust, F characteristics was conducted. Fig. 10 shows the measurement setup of the static thrust, F of the SSRLSM. For the static thrust, F measurement, each phase of the SSRLSM; Phase A, Phase B, and Phase C is measured individually. By using DC power supply, the excitation current, I was varied from 1.0 A to 5.0 A with 1.0 A increment. The SSRLSM was moved up and down by using an electrical jack. The thrust, F measured was then tabulated and plotted for comparison and verification.

Fig. 11 shows the static thrust, F characteristics of the SSRLSM. The thrust profile was taken at excitation current, I of 2.5 A at Phase B. The measurement thrust, F was compared with the simulation thrust, F. In overall, Fig. 11 (a) shows that the measured thrust, F is in agreement with the simulated thrust. The maximum thrust, F recorded from the measurement is 530 N. Meanwhile, the thrust obtained from the simulation is 600 N. Based on this thrust, F profile, the maximum thrust, F obtained at each excitation current, I was identified and shown in Fig. 11 (b). It shows that thrust, F is increasing as the excitation current increases. The maximum thrust recorded at excitation current, I of 5.0 A is 1.6 kN. Since the results are from the lab-scaled

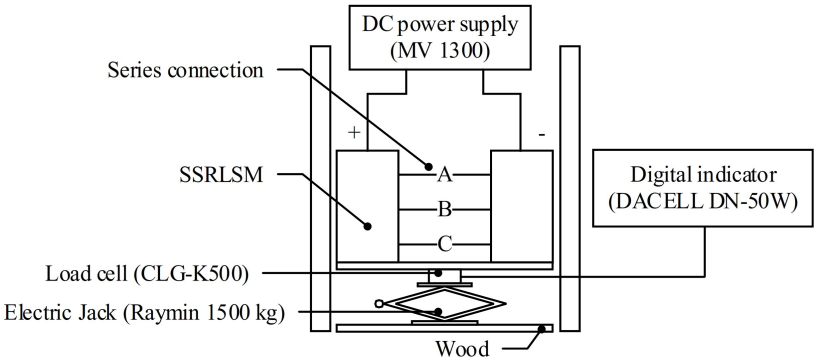

(a) Schematic diagram

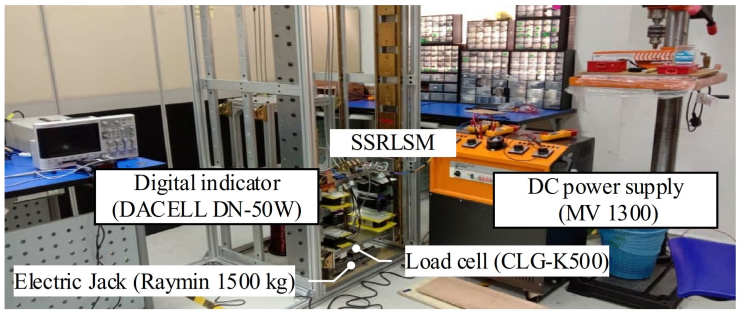

(b) Experimental setup

***Fig. 10**: SSRLSM static thrust, F measurement setup.*

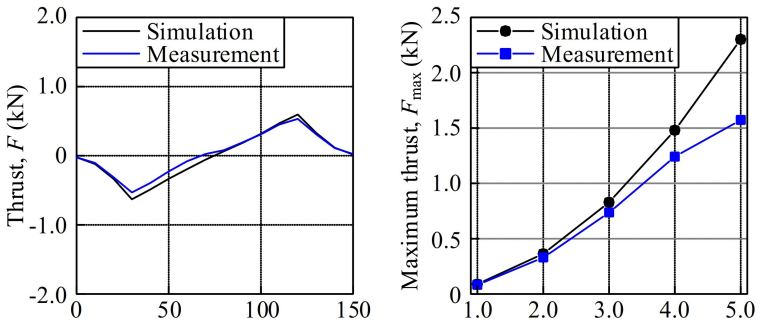

(a) Thrust, F (I = 2.5 A) (b) Maximum thrust, F_{max}

***Fig. 11**: SSRLSM thrust, F profile.*

prototype with the quarter scale of the original scale, it is expected that the full-scaled prototype will produced thrust four times higher than 1.6 kN as proved in the previous section. Therefore, the initial target of the SSRLSM for domestic lift application is expected to be achieved.

5. CONCLUSION

The SSRLSM for the domestic lift application has been designed and developed. The prototype was developed in lab scale for experimental purpose. Before developing a prototype, the SSRLSM was scaled down in terms of number of coil and stack length, z in order to study the effect of those parameters towards the SSRLSM thrust performances. Based on the simulation results, it shows that the thrust performance reduces as the number of coils and the stack length reduced. The reduction occurs in linear fashion. The thrust produces by SSRSLSM with 6-coils and stack length, z of 400 mm is 2400 N while the thrust produces by SSRSLSM with 3-coils and stack length, z of 400 mm is 1200 N. This shows that, the thrust reduced by 50 % as the number of coil reduced by half. Similar condition can be seen at variation of stack length, z where the thrust was reduced by approximately 50 % as the stack length, z reduced by half from 400 mm to 200 mm, as well as from 200 mm to 100 mm. Therefore, it can be concluded that, the thrust, F of the SSRLSM is directly proportional to the stack length, z of the SSRLSM. Apart

from that, the thrust, F was validated through thrust measurement of the SSRLSM prototype. The results show that, the simulated and measured thrust, F are agree to each other.

ACKNOWLEDGEMENT

The authors would like to thank Ministry of Education Malaysia, Universiti Teknikal Malaysia Melaka (UTeM) for providing the research grant FRGS/2018/FKE-CERIA/F00356.

REFERENCES

[1] D. Wang, Z. Feng, H. Zheng and X. Wang, "Comparative Analysis of Different Topologies of Linear Switched Reluctance Motor With Segmented Secondary for Vertical Actuation Systems," in *IEEE Transactions on Energy Conversion*, vol. 36, no. 4, pp. 2634-2645, Dec. 2021.

[2] R. Cao, E. Su and M. Lu, "Comparative Study of Permanent Magnet Assisted Linear Switched Reluctance Motor and Linear Flux Switching Permanent Magnet Motor for Railway Transportation," in *IEEE Transactions on Applied Superconductivity*, vol. 30, no. 4, pp. 1-5, June 2020.

[3] T. Hirayama, Y. Nakamori, T. Yamada and S. Kawabata, "Experimental Characterization of Linear Switched Reluctance Motor for Physical Distribution Conveyance System," *2018 21st International Conference on Electrical Machines and Systems (ICEMS)*, Jeju, Korea (South), 2018, pp. 1832-1835.

[4] B. C. Mecrow, J. W. Finch, E. A. El-Kharashi, and A. G. Jack, "Switched Reluctance Motors with Segmental Rotors," in *IEE Proceedings-Electric Power Applications*, vol. 149, no. 4, pp. 245-254, July 2002.

[5] T. R. F. Neto and R. S. T. Pontes, "Design of a Counterweight Elevator Prototype Using a Linear Motor Drive," *2007 IEEE International Electric Machines & Drives Conference*, Antalya, Turkey, 2007, pp. 376-380.

[6] M. N. Nur-Ashikin, A. S. Fairul-Azhar, M. Z. Nor-Aishah, and R. N. Firdaus, "Design of the Segmented-Type Switched Reluctance Linear Synchronous Motor (SSRLSM) for Domestic Lift Application," in *Progress In Electromagnetics Research C (PIER C),* vol. 108, pp. 13-22, Jan. 2021.

[7] K. Diao, X. Sun and M. Yao, "Robust-Oriented Optimization of Switched Reluctance Motors Considering Manufacturing Fluctuation," in *IEEE Transactions on Transportation Electrification*, vol. 8, no. 2, pp. 2853-2861, June 2022.

[8] T. Higuchi, Y. Yokoi, T. Abe, N. Yasumura, Y. Miyamoto and S. Makino, "Design analysis of a segment type linear switched reluctance motor," *2017 11th International Symposium on Linear Drives for Industry Applications (LDIA)*, Osaka, Japan, 2017, pp. 1-4.

[9] M. R. A. Calado, A. Espirito Santo, S. J. P. S. Mariano and C. M. P. Cabrita, "Characterization of a new linear switched reluctance actuator," *2009 International Conference on Power Engineering, Energy and Electrical Drives*, Lisbon, Portugal, 2009, pp. 315-320.

[10] B. Ganji and M. H. Askari, "Different topologies for linear switched reluctance motor with segmental translator," *2016 24th Iranian Conference on Electrical Engineering (ICEE)*, Shiraz, Iran, 2016, pp. 874-878.

[11] Y. Yamamoto, and H. Yamada, "Analysis of Magnetic Circuit And Starting Characteristics of Flat-Type Linear Pulse Motor With Permanent Magnets," in *T. IEE Japan*, vol. 104-B, no. 5, pp. 265–272, May 1984.

[12] C. C. Awah, O. I. Okoro, I. E. Nkan, and E. E. Okpo, "Impact of Structural Dimensions and Poles on the Torque Performance Of Dual-Stator Permanent Magnet Machines," in *Nigerian Journal of Technological Development*, vol. 19, no. 1, pp. 68-79, June 2022.

[13] D. Li, R. Qu, X. Zhang and Y. Liu, "Optimal split ratio in Switched Flux Permanent Magnet machines," *2012 IEEE Energy Conversion Congress and Exposition (ECCE)*, Raleigh, NC, USA, 2012, pp. 1925-1931.

[14] G. Yang, K. Wang and Z. Zhang, "Study on electromagnetic force ripple reduction of long stator linear synchronous motor based on unequal pole pitch," *2017 20th International Conference on Electrical Machines and Systems (ICEMS)*, Sydney, NSW, Australia, 2017, pp. 1-4.

[15] A. S. Abdel-Khalik, M. I. Masoud, S. Ahmed and A. M. Massoud, "Effect of Current Harmonic Injection on Constant Rotor Volume Multiphase Induction Machine Stators: A Comparative Study," in *IEEE Transactions on Industry Applications*, vol. 48, no. 6, pp. 2002-2013, Nov.-Dec. 2012.

[16] M. Y. Mohamed, S. A. A. Maksoud, M. Fawzi and A. E. Kalas, "Effect of poles, slots, phases number and stack length changes on the optimal design of induction motor," *2017 Nineteenth International Middle East Power Systems Conference (MEPCON)*, Cairo, Egypt, 2017, pp. 466-471.

Nur Ashikin Mohd Nasir is currently a PhD candidate in electrical engineering at the Universiti Teknikal Malaysia Melaka (UTeM). She received her B. Eng. Degree in Electrical Engineering (Power Electronics and Drives) and M. Eng. Degree in Electrical Engineering from UTeM in 2016 and 2019, respectively. The field of her research interests are power electronics, motor drives, and electrical machines..

Fairul Azhar Abdul Shukor is currently a lecturer and academic deputy dean of the Faculty of Electrical Engineering, Universiti Teknikal Melaka Malaysia (UTeM). He received his B.Eng. Degree in electrical engineering and the M.Eng. Degree in electrical power, both from Universiti Putra Malaysia (UPM) in 2002 and 2009, respectively; and his Ph.D. Degree in Electrical Machine Design from Shinshu University Nagano, Japan, in 2015. He is also a member and auditor of the Board of Engineers Malaysia and the Malaysia Board of Technologists. His research interests include the field of electrical machine design, motor drives, power electronics, and a magnetic sensor.

Norrimah Abdullah is a lecturer in Electrical Engineering Department at the Universiti Kuala Lumpur – Malaysia France Institute (UniKl - MFI), Kuala Lumpur, Malaysia. She received her B.Eng. Degree in Electrical Engineering from Universiti Malaya (UM) in 2001 and M. Sc. Degree in Instrumentation Engineering from Universiti Putra Malaysia in 2008. Currently, she is pursuing a PhD at Universiti Teknikal Melaka Malaysia UTeM. Her research interests include electrical machines, motor drives, industrial measurement and instrumentation, and magnetic sensors. .

Raja Nor Firdaus Kashfi Raja Othman is the Associate Professor at the Faculty of Electrical Engineering Department, Universiti Teknikal Melaka Malaysia (UTeM), since 2014. He received the B.Eng., M.Sc., and PhD Degrees in Electrical Power Engineering from Universiti Putra Malaysia (UPM) in 2006, 2009 and 2013, respectively. His research interest includes the field of applied magnetics, electrical machines, magnetic sensor and drives.